Proc. Natl. Acad. Sci. USA
Vol. 94, pp. 14406–14411, December 1997
Biochemistry

Chemical complementation identifies a proton acceptor for redox-active tyrosine D in photosystem II

SUNYOUNG KIM, JIE LIANG, AND BRIDGETTE A. BARRY*

Department of Biochemistry, College of Biological Sciences, University of Minnesota, St. Paul, MN 55108-1022

Communicated by Elizabeth Gantt, University of Maryland, College Park, MD, October 27, 1997 (received for review August 11, 1997)

ABSTRACT **Through the use of site-directed mutagenesis and chemical rescue, we have identified the proton acceptor for redox-active tyrosine D in photosystem II (PSII). Effects of chemical rescue on the tyrosyl radical were monitored by EPR spectroscopy. We also have acquired the Fourier–transform infrared (FT-IR) spectrum associated with the oxidation of tyrosine D and concomitant protonation of the acceptor. Mutant and isotopically labeled PSII samples are used to assign vibrational lines in the 3,600–3,100 cm^{-1} region to N-H modes of His-189 in the D2 polypeptide. When His-189 in D2 is changed to a leucine (HL189D2) in PSII, dramatic alterations of both EPR and FT-IR spectra are observed. When imidazole is introduced into HL189D2 samples, results from both EPR and FT-IR spectroscopy argue that imidazole is functionally reconstituted into an accessible pocket and that imidazole acts as a chemical mimic for His-189. Small perturbations of EPR and FT-IR spectra are consistent with access to this pocket in wild-type PSII, as well. Structures of the analogous site in bacterial reaction centers suggest that an accessible pocket, large enough to contain imidazole, is bordered by tyrosine D and His-189 in the D2 polypeptide. These data provide evidence that His-189 in the D2 polypeptide of PSII acts as a proton acceptor for redox-active tyrosine D and that proton transfer to the imidazole ring facilitates the efficient oxidation/reduction of tyrosine D.**

Tyrosine residues have low oxidation potentials (1, 2) and are used as redox-active groups in several enzymes, including ribonucleotide reductase (3, 4), photosystem II (PSII) (5–7), and prostaglandin H synthase (8). Redox-active tyrosines are postulated to facilitate long-range electron transfer reactions in some of these enzymes (9). Elucidation of the functional role of neutral tyrosine radicals, from an energetic perspective, requires identification of the proton accepting group. Alteration of the identity and pKa of this base is a method by which enzymes can adjust oxidation potentials of redox-active tyrosines and thus modify electron transfer rates.

The core of PSII, a multisubunit protein catalyzing light-driven oxidation of water and reduction of plastoquinone, is a heterodimer of the D1 and D2 polypeptides (10). The enzyme complex contains a stable, light-induced tyrosine radical, D•. Tyrosine D is residue 160 of the D2 subunit (11, 12) and forms a neutral (5), hydrogen-bonded (13–18) radical. The oxidized form of tyrosine D gives rise to a characteristic EPR signal; the *g* value of this signal is consistent with deprotonation of the tyrosine upon oxidation (5). The phenolic proton of D was postulated to be hydrogen-bonded to a neighboring basic amino acid (11, 19). In modeling studies, the conserved His-189 of the D2 polypeptide was suggested to point into a cavity occupied by tyrosine D (20, 21). Magnetic resonance experiments show that His-189 is hydrogen bonded to D• (15, 18, 22, 23).

Understanding the energetics of this redox-active tyrosine requires identification of the proton acceptor. To observe the proton acceptor for tyrosine D• directly, we have used difference Fourier-transform infrared (FT-IR) spectroscopy (24). Because the oxidation of D is light-induced (25), a double-difference spectrum, reflecting D• – D, can be acquired, as previously described. If the imidazole ring of histidine is reversibly protonated and deprotonated on alteration of the tyrosine redox state (19), the vibrational spectrum associated with the protonation of imidazole also will contribute to the double-difference spectrum (Fig. 1*A*). Unique vibrational modes from the imidazolium ion will contribute positive lines to the spectrum, whereas vibrations associated with imidazole will contribute negative lines.

Ligand replacement studies on other enzymes, for example, carbonic anhydrase (26), heme-containing proteins (27–30), and the bacterial reaction center (31), suggest a biochemical method by which the proton acceptor of tyrosine D can be identified. In the above investigations, a histidine residue was replaced with glycine or alanine by site-directed mutagenesis. Imidazole and its analogs then were reconstituted into the cavity generated in the mutated protein. In some cases, the reconstituted compounds were found to mimic the role of the removed histidine. Such an approach tests the function of the chemical mimic directly, even in a background that may contain pleotropic structural changes induced by mutagenesis. This method also allows systematic exploration of the functional impact of size, basicity, and hydrophobicity of the base. In this report, we use imidazole replacement to test the hypothesis that His-189 in the D2 polypeptide is a proton acceptor for tyrosine D.

MATERIALS AND METHODS

Cyanobacterial Culture Growth, Isotopic Labeling, and Protein Purification. The His-189D2 mutants, obtained from R. Debus (University of California, Riverside), were constructed and verified (32). Cyanobacterial strains were grown photoheterotrophically (33). $^{13}C(6)$-labeling of tyrosines (5), global ^{15}N-labeling (16), and ^{2}H exchange (16) of wild-type PSII were performed as described.

For each *Synechocystis* strain, material from several carboys was pooled at the MonoQ purification step of PSII (16, 34). The PSII yield from the HL189D2 strain was lower than wild type; the amount of PSII per 15 liters of HL189D2 cells was roughly 30 μg of chlorophyll (chl). Approximately 450 liters of HL189D2 cells were used to obtain and replicate the results described here. The HG189D2 mutant was very unstable and unsuitable for these manipulations.

The publication costs of this article were defrayed in part by page charge payment. This article must therefore be hereby marked "*advertisement*" in accordance with 18 U.S.C. §1734 solely to indicate this fact.

Abbreviations: chl, chlorophyll; D, tyrosine 160 in the D2 polypeptide of photosystem II; FT-IR, Fourier–transform infrared; PSII, photosystem II; Z, tyrosine 161 in the D1 polypeptide of photosystem II.

*To whom reprint requests should be addressed. e-mail: barry@biosci.cbs.umn.edu.

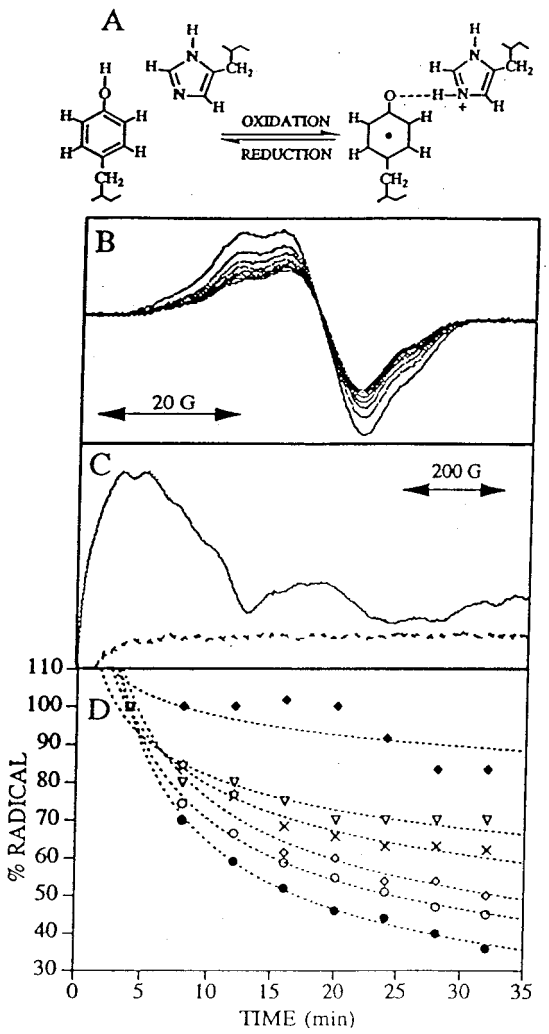

FIG. 1. (*A*) Schematic representation of a proton acceptor for the neutral tyrosine radical D•. (*B*) Tyrosine D• EPR spectra of manganese-depleted, wild-type PSII preparations recorded at pH 7.5 and −9°C. Samples were illuminated for 4 min, and successive spectra were recorded every 4 min after illumination to monitor the radical decay rate (solid lines). (*C*) Light-minus-dark EPR spectra of Q_A^- Fe^{+2} in *Synechocystis* PSII preparations. Light-minus-dark EPR spectra (dark adapted for 4 min and illuminated at −9°C for 4 min) were obtained on manganese-depleted PSII preparations at pH 7.5 containing 3 mM ferricyanide and 3 mM ferrocyanide (dotted line) and, as a positive control, oxygen evolving PSII preparations containing three equivalents of ferricyanide (solid line). (*D*) Decay of tyrosine D• EPR signal in *Synechocystis* PSII preparations. Tyrosine D• EPR spectra were recorded every 4 min; spin quantitations via double-integration of each spectra were plotted as a function of time. Data plotted are from wild type (closed circles), HQ189D2 (crosses), HL189D2 (filled diamonds), HL189D2 after imidazole reconstitution (open diamonds), HL189D2 after 4-methylimidazole reconstitution (open triangles), and wild type after imidazole reconstitution (open circles). The first spectrum recorded 4 min after illumination was normalized to 100% for each data set. Best fits to the data points are shown in dotted lines.

Chl concentrations were determined in methanol (35). Before manganese removal, HQ189D2, HL189D2, and wild-type PSII preparations had oxygen rates (33) of 1,800, 1,200, and 2,400 μmol O_2/mg chl-hr, respectively.

Manganese Depletion. Samples were depleted of manganese by using freshly prepared hydroxylamine (16). The concentrated sample then was dialyzed (molecular weight cutoff, 6,000–8,000) against 5 mM Hepes-NaOH, pH 7.5, for 12 hr. After concentration to 1 mg chl/ml, samples were divided into aliquots, flash-frozen with liquid nitrogen, and stored at −80°C until use.

Imidazole Replacement in PSII Preparations. Pooled HL189D2 PSII preparations were divided into thirds. The first third of the sample was NH_2OH-treated and then washed to remove NH_2OH (36). The sample was eluted from the MonoQ column with a buffer (33) containing 15 mM imidazole. This imidazole-treated sample was dialyzed against 5 mM Hepes·NaOH, pH 7.5 and 1 mM imidazole. The second third of the HL189D2 preparation was treated in a similar manner by using 4-methylimidazole. The last third of the HL189D2 preparation, which served as the control, was NH_2OH-treated, washed on the MonoQ column, and dialyzed against 5 mM Hepes-NaOH, pH 7.5. All three treatments were performed on the same day with the same hydroxylamine stock solution. ^{15}N-imidazole was not used; the cost of the isotopomer for a single trial would exceed $20,000.

EPR Spectroscopy. Samples were dried on mylar strips (37) with 80 μg of chl, 3 mM ferricyanide, and 3 mM ferrocyanide. Tyrosyl radical spectra were obtained, and illumination was provided as described (33, 38). Spectral conditions were: frequency, 9.1 GHz; power, 1.3 mW; modulation amplitude, 5 G; scan time, 4 min; time constant, 2 s; temperature, −9 ± 1°C. $Q_A^-Fe^{2+}$ EPR spectra were obtained as described (25). Conditions were: microwave frequency, 9.44 GHz; power, 40 mW; modulation amplitude, 32 G; scan time, 336 s; time constant, 328 ms; temperature, 4.3 ± 0.2 K.

Difference FT-IR Spectroscopy on PSII. Each manganese-depleted PSII sample, containing 25–30 μg of chl, 3 mM ferricyanide, and 3 mM ferrocyanide, was dried (16, 37); samples and conditions for drying EPR and IR samples were identical, except for the solid substrate. Absorbance in the 3,500–3,000 cm^{-1} and amide II regions of the infrared spectrum was always less than 0.55 and 0.35, respectively. Illumination was provided, and data were collected as described (24), except that a Nicolet Magna II spectrometer was used. Spectral conditions were: resolution, 4 cm^{-1}; mirror velocity, 2.5 cm/sec; Happ-Ganzel apodization; one level of zero filling; temperature, −9°C. Double-sided interferograms were collected, and 425 scans taken in 4 min were coadded for each interferogram. Data recorded in the light were ratioed directly to data recorded in the dark. Spectra were normalized to the amide II absorbance or to the protein concentration; these methods gave equivalent results. The data shown are the average of 8–21 spectra.

Computer Modeling. Identification and accurate computation of pockets were performed by using an alpha shape-based pocket method (39). This method is based on the alpha shape, the weighted Delaunay triangulation, and the discrete flow method from computational geometry and algebraic topology (see ref. 39 and references therein). A subset of the organized Delaunay tetrahedra, spanning atomic centers, corresponds mathematically to cavities and pockets in molecules and can be mapped rigorously onto the molecular surface.

RESULTS

In Fig. 1, we present EPR spectra of manganese-depleted, wild-type *Synechocystis* PSII complexes (33). Upon illumination, both Z• (tyrosine 161 in the D1 polypeptide of PSII) and D• are produced, and the slow decay of D• then can be monitored in successive 4-min scans following illumination (Fig. 1*B*). Monitoring the production of the $Q_A^-Fe^{+2}$ EPR signal shows that these illumination conditions do not result in the detectable stable reduction of Q_A (Fig. 1*C*). Fluorescence measurements support this conclusion; Q_B is not functional in this preparation (data not shown).

When His-189 in the D2 polypeptide is changed to a glutamine (HQ189D2) or a leucine (HL189D2), there is a change in the D• EPR lineshape in our samples (data to be published elsewhere); such alterations have been described previously (15, 18, 22). These resultant changes in the EPR

lineshape may be caused by differences in tyrosyl radical structure, induced by changes in the local protein environment, or caused by the oxidation of chl, instead of the tyrosine, in a small number of centers. In HL189D2, we also observe a decrease in radical yield (Table 1). In HL189D2 and HQ189D2, there is a decrease in the rate of radical decay (Table 1 and Fig. 1*D*, filled diamonds and crosses). Treatment of HL189D2 PSII with imidazole increases both radical yield (Table 1) and the rate of decay of the radical (Fig. 1*D*, empty diamonds), with no large effect on radical lineshape (data not shown). Because the radical decay rate accelerates to near the wild-type decay rate on addition of imidazole to HL189D2 PSII, these results imply that the reconstituted imidazole assumes the function of the removed histidine. An imidazole analog, 4-methylimidazole, which has a higher pKa (40) and larger volume, is not as effective as imidazole in increasing the yield or decay rate of the radical (Table 1 and Fig. 1*D*, empty triangles). The presence of imidazole in wild-type samples slightly alters the yield and slightly slows the decay rate of tyrosine D• (Table 1 and Fig. 1*D*, empty circles).

To investigate the nature of the interaction between imidazole and tyrosine D, we have used difference FT-IR spectroscopy. A methodology to obtain double-difference FT-IR spectra reflecting contributions from D•−D has been reported (24). By using 90- and 4-min dark adaptations, two light-minus-dark difference spectra, reflecting D•Z•−DZ and D•Z•−D•Z, are produced. Construction of the double-difference spectrum, in which the above spectra are directly subtracted, on a one-to-one basis, emphasizes contributions from the tyrosine D and its relatively dark-stable radical. These spectra will be sensitive to changes in the structure of the tyrosine upon oxidation, as well as to coupled alterations in the protein environment. It also should be noted that there are expected to be no detectable contributions from cytochrome *b*-559 or Q_A^- (S.K. and B.A.B., unpublished results and refs. 32 and 41-43) in these spectra.

In Fig. 2*A* (solid line), we present the 3,600–3,100 cm^{-1} region of the infrared spectrum associated with oxidation of D in wild-type PSII. A complex pattern of negative and positive lines between 3,350 and 3,250 cm^{-1} is observed. These lines are absent in a mutant PSII (Fig. 2*A*, dotted line), in which redox-active tyrosine D is changed to a nonredox-active phenylalanine (YF160D2). This result shows that the structural change, giving rise to this vibrational signature, is dependent on electron transfer reactions involving tyrosine D. $^{13}C(6)$ labeling of tyrosine has no significant effect on frequencies in this region (data not shown), arguing that these vibrational modes do not arise from C-H vibrational modes of the D tyrosine.

Protonation of histidine would be expected to perturb the frequencies and intensities of N-H stretching modes. N-H stretching vibrations would be expected in the 3,500 cm^{-1} region; this possible origin for the vibrational lines between 3,350 and 3,250 cm^{-1} can be tested by ^{15}N labeling and ^{2}H exchange (44–46). Upon global ^{15}N labeling (16), negative lines at 3,349 and 3,251 cm^{-1} downshift to 3,339 and 3,241 cm^{-1}, whereas positive lines at 3,300 and 3,270 cm^{-1} downshift to 3,290 and 3,260 cm^{-1} (Fig. 2*B*). A 10-cm^{-1} downshift is in reasonable agreement with the 8-cm^{-1} downshift expected for a harmonic N-H stretching mode and for the N-H stretching mode of imidazole (46). Deuterium exchange shows that vibrational lines between 3,349–3,251 cm^{-1} (Fig. 2*C*) downshift to 2,600–2,400 cm^{-1} (Fig. 2*D*). This downshift of a factor of 1.3 upon ^{2}H exchange is in reasonable agreement with the expected value of 1.4 for a harmonic N-H stretching mode. The above data argue that the vibrational lines between 3,350–3,250 cm^{-1} are N-H stretching motions arising from an amino acid residue.

Table 1. Relative spin quantitations of the tyrosine D• radical in different PSII samples

Sample	4-min dark adaptation	32-min dark adaptation
Wild type	100	42
HQ189D2	97	67
HL189D2	17	17
HL189D2 + Im	38	23
HL189D2 + 4-MeIm	27	21
Wild type + Im	136	65

The standard error is approximately 15%.

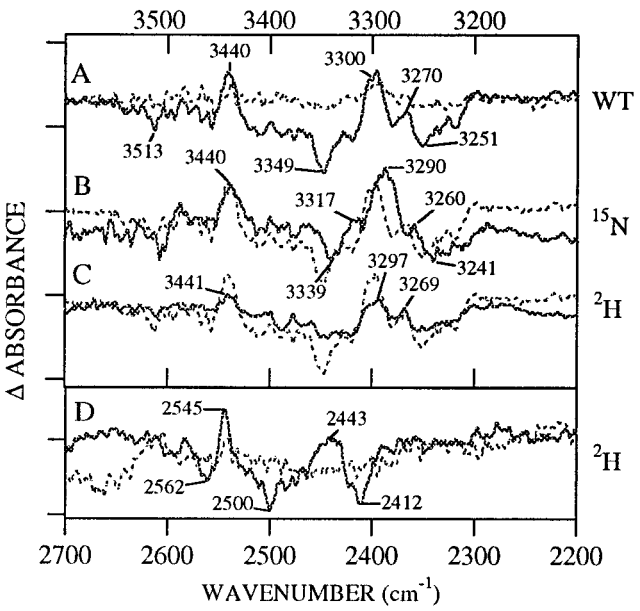

FIG. 2. Difference D• − D FT-IR spectra in manganese-depleted *Synechocystis* PSII preparations at pH 7.5. The spectra shown in solid lines were obtained from (*A*) wild type, (*B*) ^{15}N-labeled wild type, and (*C* and *D*) $^{2}H_2O$-exchanged wild type. Superimposed in the dotted line in *A* is a spectrum obtained from the YF160D2 mutant. Superimposed in the dotted line in *B–D* is the wild-type spectrum. Tick marks on the *y* axis correspond to 1×10^{-4} (*Upper*) and 2×10^{-5} (*Lower*) AU.

The HQ189D2 mutant was used to identify the amino acid residue, which contributes to the double-difference spectrum in the 3,500 cm^{-1} region. In Figs. 3*A* and 4*A*, we present two regions from the FT-IR spectrum obtained from HQ189D2 PSII. Lines in the 1,800–1,350 cm^{-1} region have been assigned to His-189, D•, and D based on isotopic labeling experiments (data not shown). Although Fig. 4*A* shows that intense spectral features are observed in the 1,800–1,350 cm^{-1} region of spectra obtained on HQ189D2 PSII samples, Fig. 3*A* shows that this mutation eliminates the N-H stretching vibrations in the 3,300 cm^{-1} region. These results support the assignment of these spectral features to N-H stretching vibrations of the imidazole ring in His-189.

Mutagenesis of His-189 to leucine eliminates spectral features in the 3,300 cm^{-1} region (Fig. 3*B*), consistent with the yield and decay rate of the radical (Table 1 and Fig. 1*D*), and produces a spectrum resembling the YF160D2 spectrum (data not shown) between 1,800 and 1,350 cm^{-1} (Fig. 4*B*). Observed spectral features in the 1,800–1,350 cm^{-1} region may arise from the production of a narrow radical, possibly a chl cation radical, in a small number of centers (11). When HL189D2 is reconstituted with imidazole, a complex feature centered at 3,300 cm^{-1}, similar, but not identical, to the wild-type spectrum, is recovered (Fig. 3*C*). In the 1,800–1,350 cm^{-1} region (Fig. 4*C*), treatment of HL189D2 PSII with imidazole results in a spectrum with new, complex spectral features, which do not closely resemble the spectral features observed in wild type. Use of 4-methylimidazole has a smaller effect on the

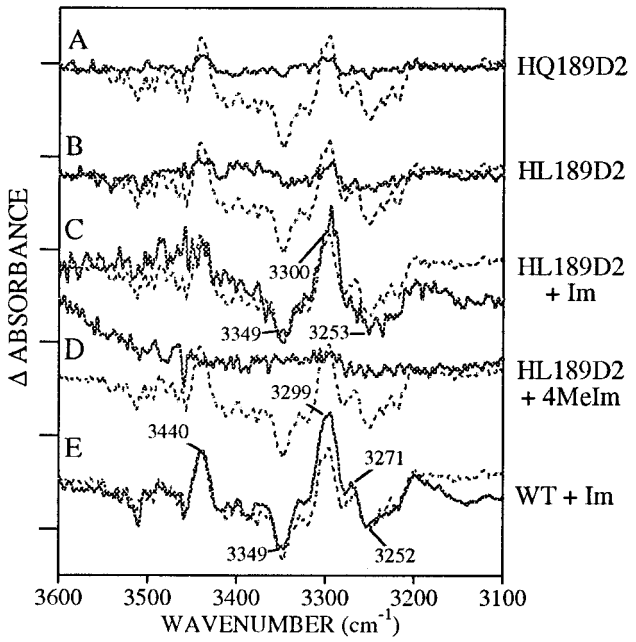

FIG. 3. Difference D• − D FT-IR spectra in manganese-depleted *Synechocystis* PSII preparations at pH 7.5. The spectra shown in solid lines were obtained from (*A*) HQ189D2, (*B*) HL189D2, (*C*) HL189D2 after treatment with imidazole, (*D*) HL189D2 after treatment with 4-methylimidazole, and (*E*) wild type after treatment with imidazole. Superimposed in the dotted line in *A–E* is the wild-type spectrum. Tick marks on the *y* axis correspond to 1×10^{-4} absorbance units.

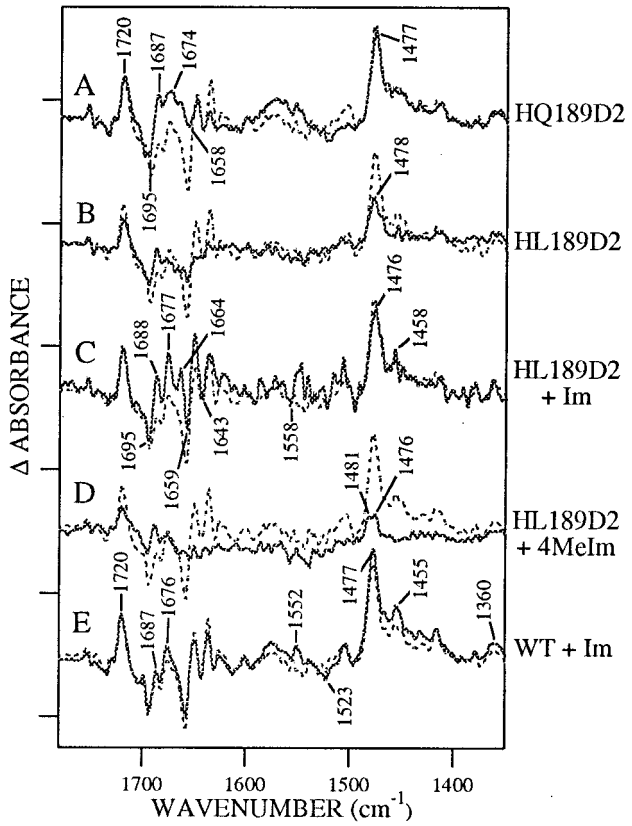

FIG. 4. Difference D• − D FT-IR spectra in manganese-depleted *Synechocystis* PSII preparations at pH 7.5. Spectra shown in the solid lines were obtained from (*A*) HQ189D2, (*B*) HL189D2, (*C*) HL189D2 after treatment with imidazole, (*D*) HL189D2 after treatment with 4-methylimidazole, and (*E*) wild type after treatment with imidazole. Superimposed in the dotted line in *A–E* is the wild-type spectrum. Tick marks on the *y* axis correspond to 2×10^{-4} absorbance units.

infrared spectrum, when compared with imidazole (Figs. 3*D* and 4*D*). Finally, treatment of control PSII with imidazole has either a small or negligible effect on spectral intensities and frequencies (Figs. 3*E* and 4*E*).

To obtain more information about the accessibility of imidazole into pockets near tyrosine D in wild-type and mutant PSII, we have examined the bacterial reaction center from purple nonsulfur bacteria. This reaction center was the first membrane protein to yield an atomic resolution structure (47). The analogous residues for D and His-189 in the D2 polypeptide of PSII are Arg-164 and His-193 in the M subunit of *Rhodobacter sphaeroides* (21). Analysis for surface-accessible pockets by using the alpha-shape method shows that all available *R. sphaeroides* structures have significant surface pockets containing both R164 and H193 (Fig. 5). The pocket is slightly variable in size. The smallest cavity is lined by 25 atoms from nine residues (48), whereas the largest cavity is lined by 52 atoms from 23 residues (49). The relevance of this modeling to PSII is strengthened because the majority of the cavity atoms come from residues in regions that exhibit 47–67% similarity upon comparison of D2 sequences from cyanobacteria, spinach and pea with the M sequence from *R. sphaeroides*. This sequence homology will be discussed in detail in a future publication.

DISCUSSION

Our EPR experiments have shown that either reconstituted imidazole or the native His-189 of the D2 polypeptide increases the yield and decay rate of tyrosyl radical, D•. Our vibrational spectra show that imidazole and His-189 contribute to the FT-IR spectrum associated with the oxidation of tyrosine D. Such a contribution can occur because imidazole and histidine undergo a reversible structural change, such as a protonation, that is coupled to the electron transfer reactions (Fig. 1*A*). In the N-H stretching region, the lines assignable to reconstituted imidazole and to native histidine are similar in frequency. The observed infrared spectral changes are consistent with protonation of imidazole and histidine in imidazole-rescued HL189D2 and in wild-type PSII, respectively (44–46). Modeling leads to the expectation that a conserved surface-accessible pocket is located near tyrosine D. This result predicts that imidazole will have access to tyrosine D in HL189D2. Therefore, we conclude that His-189 is the proton acceptor for tyrosine D and that in the absence of His-189, imidazole can chemically complement the function of this histidine (Fig. 1*A*).

We have attributed the effect of imidazole on HL189D2 PSII to a direct functional role for imidazole in electron transfer-linked proton transfer. However, another possible explanation is that imidazole plays a structural role. In this second scenario, imidazole itself is not protonated, but its addition permits the protonation of another site in the protein. Observed similarities between the electron transfer rates and the 3,350–3,250 cm^{-1} regions of the FT-IR spectrum, when imidazole-rescued and wild-type samples are compared, cause us to favor the first possible explanation over the second.

On the other hand, our results show that 4-methylimidazole is either too large to fit into the cavity or too basic (40) to act as an efficient, reversible proton acceptor and chemical mimic in PSII. When wild-type PSII is treated with imidazole, our data suggest that imidazole does not have efficient access to the tyrosyl radical, but can be protonated in a number of reaction centers. This protonation now competes with efficient protonation of histidine and leads to small changes in the radical decay rate and in yield. We do not expect the wild-type pocket to be readily accessible to charged species (50) without

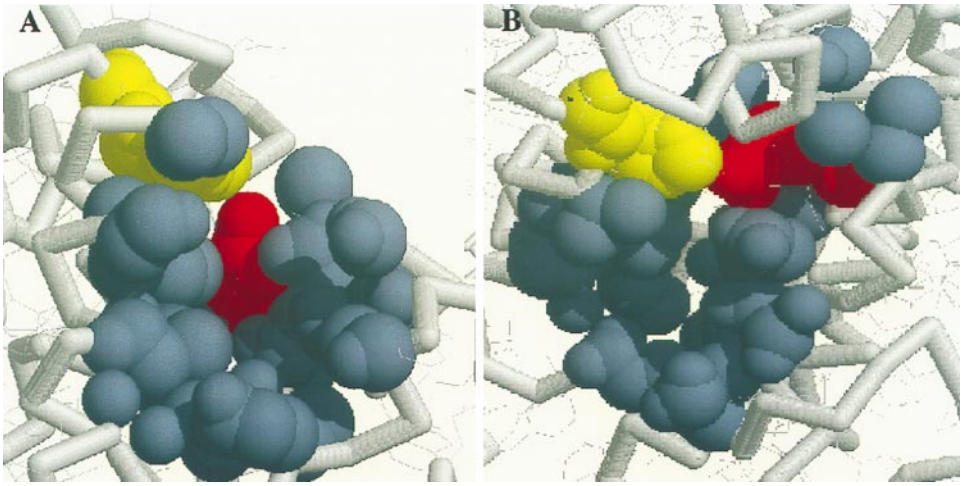

FIG. 5. Models of the analogous residues to tyrosine D (red) and His-189 (yellow) of D2 in the bacterial reaction centers *R. sphaeroides*. The atoms in blue-gray define atom spheres bounding a surface-accessible pocket. The models in *A* and *B* are related by rotation.

the use of the column chromatography-based exchange methods used here.

The conclusion that imidazole is reversibly protonated in PSII is based on comparison with previous investigations, which have reported vibrational modes of the protonated and unprotonated species (44–46, 51–54). This work and our own data on the protonation of imidazole *in vitro* (data not shown) predict that the protonation spectrum will exhibit vibrational modes in the 3,400–3,100 cm^{-1} and the 1,800–1,350 cm^{-1} regions. On addition of imidazole to HL189D2 PSII (Fig. 3*C*), the center frequency for the N-H stretch is approximately 3,300 cm^{-1}. For imidazole *in vitro*, vibrational lines between 3,300 and 3,100 cm^{-1} are assigned to the N-H stretching mode of molecules that are hydrogen-bonded (44, 45, 51). For example, hydrogen bonding of imidazole to dioxane gives a N-H stretching mode at 3,305 cm^{-1} (45). Thus, the 3,300 cm^{-1} frequency of the N-H stretching mode in imidazole-rescued HL189D2 PSII is consistent with hydrogen bonding of reconstituted imidazole to an oxygen, such as the phenolic oxygen of tyrosine. As previously described, there also can be contributions from C-H stretching modes and Fermi resonances in this region (45); such a contribution complicates spectral interpretation.

When His-189 is protonated in wild-type PSII (Fig. 2*A*), a more complex set of spectral contributions in the 3,350–3,250 cm^{-1} region is observed, compared with imidazole-reconstituted HL189D2 PSII. Increased complexity is consistent with the decrease in molecular symmetry (51–54). The frequencies of spectral features are similar, when wild-type and imidazole-rescued PSII are compared. Analysis of EPR intensities and decay rates and of these infrared spectra implies that imidazole, which has been reconstituted into HL189D2 PSII, has a larger infrared molar absorptivity, when compared with histidine. This outcome is possible, because infrared intensities for secondary amines are known to be extensively influenced by chemical substitution (55), changes in polarity (55), and hydrogen bonding (45).

Although the 3,350–3,250 cm^{-1} regions of wild-type and imidazole-reconstituted PSII are similar, dramatic spectral differences are observed in the 1,800–1,350 cm^{-1} region. The variation observed in the ring stretching and N-H bending modes in the 1,800–1,350 cm^{-1} region (44–46, 51–54) may be caused by environmental heterogeneity affecting the spectrum of imidazole, which is not rigidly bound. The N-H stretching modes in the 3,350–3,250 cm^{-1} spectral region of both imidazole and histidine are substantially broader than the lines in the 1,800–1,350 cm^{-1} region, and, thus, these vibrational modes may be less sensitive to these effects. Note that imidazole may contribute throughout the 1,800–1,350 cm^{-1} spectrum, even in regions dominated by tyrosyl radical and tyrosine vibrational modes in wild-type PSII.

An interesting and unexpected observation to emerge from our measurements is the effect of the proton acceptor on electron transfer rates. In the absence of His-189, addition of imidazole accelerates the decay rate of the radical. These results imply an interaction between proton and electron transfer and suggest that proton transfer is a requirement for efficient electron transfer involving tyrosine D. We will test the hypothesis that proton and electron transfer reactions are coupled in this fashion in future work.

We thank Drs. M. Schiffer, D. Hanson, and C. Woodward for helpful discussions, Dr. C. Woodward for support of J.L., and Dr. M. Razeghifard for assistance with the cryogenic EPR measurements. This work was supported by National Institutes of Health GM 43273 (to B.A.B).

1. Harriman, A. (1987) *J. Phys. Chem.* **91,** 6102–6104.
2. DeFelippis, M. R., Murphy, C. P., Faraggi, M. & Klapper, M. H. (1989) *Biochemistry* **28,** 4847–4853.
3. Graslund, A., Ehrenberg, A. & Thelander, L. (1982) *J. Biol. Chem.* **257,** 5711–5715.
4. Larsson, A. & Sjoberg, B.-M. (1986) *EMBO J.* **5,** 2037–2040.
5. Barry, B. A. & Babcock, G. T. (1987) *Proc. Natl. Acad. Sci. USA* **84,** 7099–7103.
6. Boerner, R. J. & Barry, B. A. (1993) *J. Biol. Chem.* **268,** 17151–17154.
7. Boerner, R. J. & Barry, B. A. (1994) *J. Biol. Chem.* **269,** 134–137.
8. Smith, W. L., Eling, T. E., Kulmacz, R. J., Marnett, L. J. & Tsai, A.-L. (1992) *Biochemistry* **31,** 3–7.
9. Barry, B. A. (1993) *Photochem. Photobiol.* **57,** 179–188.
10. Nanba, O. & Satoh, K. (1987) *Proc. Natl. Acad. Sci. USA* **84,** 109–112.
11. Debus, R. J., Barry, B. A., Babcock, G. T. & McIntosh, L. (1988) *Proc. Natl. Acad. Sci. USA* **85,** 427–430.
12. Vermaas, W. F. J., Rutherford, A. W. & Hansson, O. (1988) *Proc. Natl. Acad. Sci. USA* **85,** 8477–8481.
13. Rodriguez, I. D., Chandrashekar, T. K. & Babcock, G. T. (1987) in *Progress in Photosynthesis Research*, ed. Biggins, J. (Martinus Nijhoff, Dordrecht, The Netherlands), Vol. I, pp. 471–473.
14. Evelo, R. G., Dikanov, S. A. & Hoff, A. J. (1989) *Chem. Phys. Lett.* **157,** 25–30.
15. Tang, X.-S., Chisholm, D. A., Dismukes, G. C., Brudvig, G. W. & Diner, B. A. (1993) *Biochemistry* **32,** 13742–13748.
16. Bernard, M. T., MacDonald, G. M., Nguyen, A. P., Debus, R. J. & Barry, B. A. (1995) *J. Biol. Chem.* **270,** 1589–1594.
17. Force, D. A., Randall, D. W., Britt, R. D., Tang, X.-S. & Diner, B. A. (1995) *J. Am. Chem. Soc.* **117,** 12643–12644.
18. Un, S., Tang, X.-S. & Diner, B. A. (1996) *Biochemistry* **35,** 679–684.

19. Babcock, G. T., Barry, B. A., Debus, R. J., Hoganson, C. W., Atamian, M., McIntosh, L., Sithole, I. & Yocum, C. F. (1989) *Biochemistry* **28,** 9557–9565.
20. Svensson, B., Vass, I., Cedergren, E. & Styring, S. (1990) *EMBO J.* **7,** 2051–2059.
21. Ruffle, S. V., Donnelly, D., Blundell, T. L. & Nugent, J. H. A. (1992) *Photosyn. Res.* **34,** 287–300.
22. Tommos, C., Davidsson, L., Svensson, B., Madsen, C., Vermaas, W. & Styring, S. (1993) *Biochemistry* **32,** 5436–5441.
23. Campbell, K. A., Peloquin, J. M., Diner, B. A., Tang, X.-S., Chisholm, D. A. & Britt, R. D. (1997) *J. Am. Chem. Soc.* **119,** 4787–4788.
24. MacDonald, G. M., Bixby, K. A. & Barry, B. A. (1993) *Proc. Natl. Acad. Sci. USA* **90,** 11024–11028.
25. Miller, A.-F. & Brudvig, G. W. (1991) *Biochim. Biophys. Acta* **1056,** 1–18.
26. Tu, C. & Silverman, D. N. (1989) *Biochemistry* **28,** 7913–7918.
27. Barrick, D. (1994) *Biochemistry* **33,** 6546–6554.
28. Fitzgerald, M. N., Churchill, M. J., McRee, D. E. & Goodin, D. B. (1994) *Biochemistry* **33,** 3807–3818.
29. Decatur, S. M. & Boxer, S. G. (1995) *Biochemistry* **34,** 2122–2129.
30. Wilks, A., Sun, J., Loehr, T. M. & Ortiz de Montellano, P. R. (1995) *J. Am. Chem. Soc.* **117,** 2925–2926.
31. Goldsmith, J. O., King, B. & Boxer, S. G. (1996) *Biochemistry* **35,** 2421–2428.
32. Boerner, R. J., Bixby, K. A., Nguyen, A. P., Noren, G. H., Debus, R. J. & Barry, B. A. (1993) *J. Biol. Chem.* **268,** 1817–1823.
33. Barry, B. A. (1995) *Methods Enzymol.* **258,** 303–319.
34. Noren, G. H., Boerner, R. J. & Barry, B. A. (1991) *Biochemistry* **30,** 3943–3950.
35. Lichtenthaler, H. K. (1987) *Methods Enzymol.* **148,** 350–382.
36. Peiffer, W. E., Ingle, R. T. & Ferguson-Miller, S. (1990) *Biochemistry* **29,** 8696–8701.
37. MacDonald, G. M. & Barry, B. A. (1992) *Biochemistry* **31,** 9848–9856.
38. Ma, C. & Barry, B. A. (1996) *Biophys. J.* **71,** 1961–1972.
39. Edelsbrunner, H., Facello, M. & Liang, J. (1996) in *Biocomputing: Proceedings of the 1996 Pacific Symposium*, eds. Hunter, L. & Klein, T. (World Scientific, Singapore), pp. 272–287.
40. Jiang, F., McCracken, J. & Peisach, J. (1990) *J. Am. Chem. Soc.* **112,** 9035–9044.
41. Boerner, R. J., Nguyen, A. P., Barry, B. A. & Debus, R. J. (1992) *Biochemistry* **31,** 6660–6672.
42. Noren, G. H. & Barry, B. A. (1992) *Biochemistry* **31,** 3335–3342.
43. MacDonald, G. M., Boerner, R. J., Everly, R. M., Cramer, W. A., Debus, R. J. & Barry, B. A. (1994) *Biochemistry* **33,** 4393–4400.
44. Columbo, L., Bleckmann, P., Schrader, B., Scheider, R. & Plesser, T. (1974) *J. Chem. Phys.* **61,** 3270–3278.
45. Wolff, H. & Muller, H. (1974) *J. Chem. Phys.* **60,** 2938–2939.
46. Majoube, M. & Vergoten, G. (1992) *J. Mol. Struct.* **266,** 345–352.
47. Deisenhofer, J. & Michel, H. (1989) *Science* **245,** 1463–1473.
48. Ermler, U., Fritzsch, G., Buchanan, S. K. & Michel, H. (1994) *Structure* **2,** 925–936.
49. Yeates, T. O., Komiya, H., Chirino, A., Rees, D. C., Allen, J. P. & Feher, G. (1988) *Proc. Natl. Acad. Sci. USA* **85,** 7993–7997.
50. Innes, J. B. & Brudvig, G. W. (1989) *Biochemistry* **28,** 1116–1125.
51. Garfinkel, D. & Edsall, J. T. (1958) *J. Am. Chem. Soc.* **80,** 3807–3812.
52. Caswell, D. S. & Spiro, T. G. (1986) *J. Am. Chem. Soc.* **108,** 6470–6477.
53. Harhay, G. P. & Hudson, B. S. (1993) *J. Phys. Chem.* **97,** 8158–8164.
54. Markham, L. M., Mayne, L. C., Hudson, B. S. & Zgierski, M. Z. (1993) *J. Phys. Chem.* **97,** 10319–10325.
55. Bellamy, L. J. (1980) *The Infrared Spectra of Complex Molecules* (Chapman & Hall, London) Vol. II, pp. 107–116.